Int. J. Morphol.,
44(1):121-129, 2026.

The Effectiveness of Craniometric Landmarks-Facial Landmarks for Craniofacial Superimposition Using Genetic Algorithm in a Thai Population

Eficacia de los Puntos de Referencia Craneométricos y Faciales para la Superposición Craneofacial Mediante Algoritmos Genéticos en una Población Tailandesa

Jetniphit Srisinghasongkram[1]; Patison Palee[2]; Tawachai Monum[3]; Sukon Prasitwattanaseree[4]; Anak Iamaroon[5] & Pasuk Mahakkanukrauh[6,7]

SRISINGHASONGKRAM, J.; PALEE, P.; MONUM, T.; PRASITWATTANASEREE, S.; IAMAROON, A. & MAHAKKANUKRAUH, P. The Effectiveness of craniometric landmarks-facial landmarks for craniofacial superimposition using genetic algorithm in a Thai population. *Int. J. Morphol., 44(1)*:121-129, 2026.

SUMMARY: Craniofacial superimposition has been a good forensic tool for human identification when primary identifiers such as DNA, fingerprints, or dental records are not present for human identification. Herein, a semi-automated method combines real-coded genetic algorithm and landmark-based optimization applied to 30 male and 40 female skull–face pairs. For accuracy, mean square error (MSE), area, and distance were evaluated in two landmark sets (nine and seventeen points). The nine-landmark set achieved better and more consistent findings (41.11 % among males; 38.33 % among females) than the seventeen-landmark set (40 % and 34.16 %, respectively). Area-based assessment showed the lowest value of difference and the highest accuracy, specifically with females, and MANOVA demonstrated significant differences only with males at the mandibular and zygomatic landmarks. Based on these results, a smaller set of landmarks, but more appropriate ones, increases both accuracy and computational efficiency, while area-based metrics are the most significant. Considering the limitations of two-dimensional data, however, the technique remains feasible in resource-constrained settings, supporting craniofacial superimposition as a reliable form of forensic identification.

KEY WORDS: Craniofacial superimposition; Skull; Forensic anthropology; Genetic algorithm.

INTRODUCTION

Craniofacial superimposition has been acknowledged as a progressive and reliable method for confirming identification after death using secondary data, and so is particularly relevant in forensic studies. The craniofacial superimposition model, initiated in 1867, served as the basis for the practical development (Taylor & Brown, 1998) of this technique. Originally devised for exclusion, the function of superimposition has since evolved out of necessity in order to confirm the identity of those who have died in the absence of other methods of identification (Ubelaker & Scammell, 1992). Armed with advanced forensic knowledge, criminals resort to extreme techniques including amputation, burning, mutilation and dismemberment to erase any identifiable features and disrupt identification efforts. Consequently, the difficulty is increasing for personal identification requiring increasingly advanced forensic analysis methods. The craniofacial superimposition method has been iteratively improved and enhanced by the application of computer assisted processes (Damas *et al*., 2020). Advances in imaging tools including 3D imaging and enhanced facial-craniofacial overlays have increased the precision and usability of the resulting information.

However, 3D images using craniofacial superimposition remain constrained by several factors, notably the high cost of CT scans and the limited implementation of computer-aided processing systems in

[1] PhD Program in Forensic Osteology and Odontology, Faculty of Medicine, Chiang Mai University, Chiang Mai, Thailand.
[2] Department of Digital Game, College of Arts Media and Technology, Chiang Mai, Thailand.
[3] Department of Forensic Medicine, Faculty of Medicine, Chiang Mai University, Chiang Mai, Thailand.
[4] Department of Statistics, Faculty of Science, Chiang Mai University, Chiang Mai, Thailand.
[5] Department of Oral Biology and Diagnostic Sciences, Faculty of Dentistry, Chiang Mai University, Chiang Mai, Thailand.
[6] Department of Anatomy, Faculty of Medicine, Chiang Mai University, Chiang Mai, Thailand.
[7] Excellence Center in Osteology Research and Training Center (ORTC), Faculty of Medicine, Chiang Mai University, Chiang Mai, Thailand.
FUNDING. The authors received financial support from Faculty of Medicine, Chiang Mai University (no. 091-2565) for the research, authorship and/or publication of this article.

Received: 2025-09-26 Accepted: 2025-11-24

forensic practice, particularly in resource-limited regions. In this regard, Thailand is a case study, as craniofacial superimposition methods including composite imaging have been suspended for more than twenty years due to inadequate resources and infrastructure. The first research in the field of craniofacial superimposition in Thailand was developed by Srisinghasongkram *et al*. (2019), who revived composite imaging through a combination of traditional image overlays and mathematical processing methods. This research showed a first step forward in Thailand, helping to utilize limited resources in craniofacial superimposition to more practically implementable and reliable methods in forensic work that are now using Artificial Intelligence. These technologies have introduced more refined methods for image overlay, including the use of Global Optimization to optimize the alignment of facial and craniofacial features (Yuvaraj *et al*., 2020). AI models also help tackle the difficulties of facial variability by employing advanced algorithms like curve registration (Tan *et al*., 2020), which makes sure that facial and skull attributes match more precisely. Being able to inspect correlations between critical anatomical sites has helped to drive feasibility for more refined confirmations of death.

MATERIAL AND METHOD

This study was approved by the Ethics Committee of the Faculty of Medicine, Chiang Mai University, Thailand (study code: ANA-2564-08580). A real-coded genetic algorithm, in combination with Euclidean distance and curve registration, was employed to achieve semi-automatic control of image superimposition. The software was specifically developed for 2D–2D craniofacial superimposition, incorporating operator-defined anatomical landmarks. The outputs were evaluated using mean square error, anatomical landmark distance, and area-based

Table I. Craniometric landmarks - Facial landmarks and definition.

	Craniometric landmarks		Facial landmarks	
	Landmarks	Definition	Landmarks	Definition
9 Anatomical Landmarks				
	Glabella (g)	The point between the supraorbital ridges.	Glabella (g')	The point between the eyebrows.
	Nasion (n)	The midpoint of the suture between the frontal and the two nasal bones.	Nasion (n')	The point on the anterior to the nasofrontal suture.
	Nasospinale (ns)	The point between the lower margins of the right and left nasal apertures, intersected by the midsagittal plane.	Pronasale (pn')	The most anterior point of the apex nasi.
	Prosthion (pr)	The apex of the alveolus in the midline between the maxillary central incisors.	Labiale superius (ls')	The midpoint on the vermilion line of the upper lip.
	Infradentale (id)	Median point at the superior tip of the septum between the mandibular central incisors.	Labiale inferius (li')	The midpoint on the vermilion line of the lower lip.
	Zygion (zy)	The lateral point on the zygomatic arch.	Zygion (zy')	The lateral point of the cheeks (zygomaticomalar) region.
	Alare (al)	The most lateral point on the nasal ala.	Alare (al')	The lateral point on the alar contour.
17 Anatomical Landmarks				
	Pogonion (pg)	Most anterior at median point on the mental eminence.	Pogonion (pg')	The most anterior point at the midline of chin.
	Gnathioin (gn)	The median point between pogonion and menton.	Gnathion (gn')	The median point that between pogonion and menton.
	Ectoconchion (ec)	The lateral point on the bisect transverse plane at the orbit.	Exocanthion (ex')	The most lateral point of palpebral fissure.
	Medial Orbit (mo)	The point on the anterior lacrimal crest as a same plane of ectoconchion.	Maxillo frontale (mf')	The anterior lacrimal crest at the frontomaxillary suture.
	Gonion (go)	Point at the angle of mandible.	Gonion (go')	Point at the angle of mandible.

comparison metrics. Facial and cranial specimens were obtained from the Osteology Research and Training Center, Department of Anatomy, Faculty of Medicine, Chiang Mai University. Facial images were digitized from donor history photographs using a laser scanner at a resolution of 600 dpi, restricted to frontal-plane views. Skull images were photographed by using a DSLR camera at the same angle as the donor's facial images with medical photography protocols such as lighting, background, and distance (Barut & Ertilav, 2011). The skulls were articulated following dental occlusion principles (Okeson, 2020). The study sample consisted of 30 males and 40 females, aged 35–90 years.

Anatomical landmarks for craniofacial superimposition

In this study, anatomical landmarks were based on previous research by Nickerson *et al*. (1991), Ricci *et al*. (2006), Ballerini *et al*. (2007), and Caple & Stephan (2016), and the Standards for Data Collection from Human Skeletal Remains by Buikstra & Ubelaker (1994). A total of 17 anatomical landmarks were used, classified into craniometric landmarks (Fig. 1A) and facial landmarks (Fig. 1B). Anatomical landmark selection was carried out by a craniofacial superimposition practitioner. The list of craniometric and facial landmarks is provided in Table I.

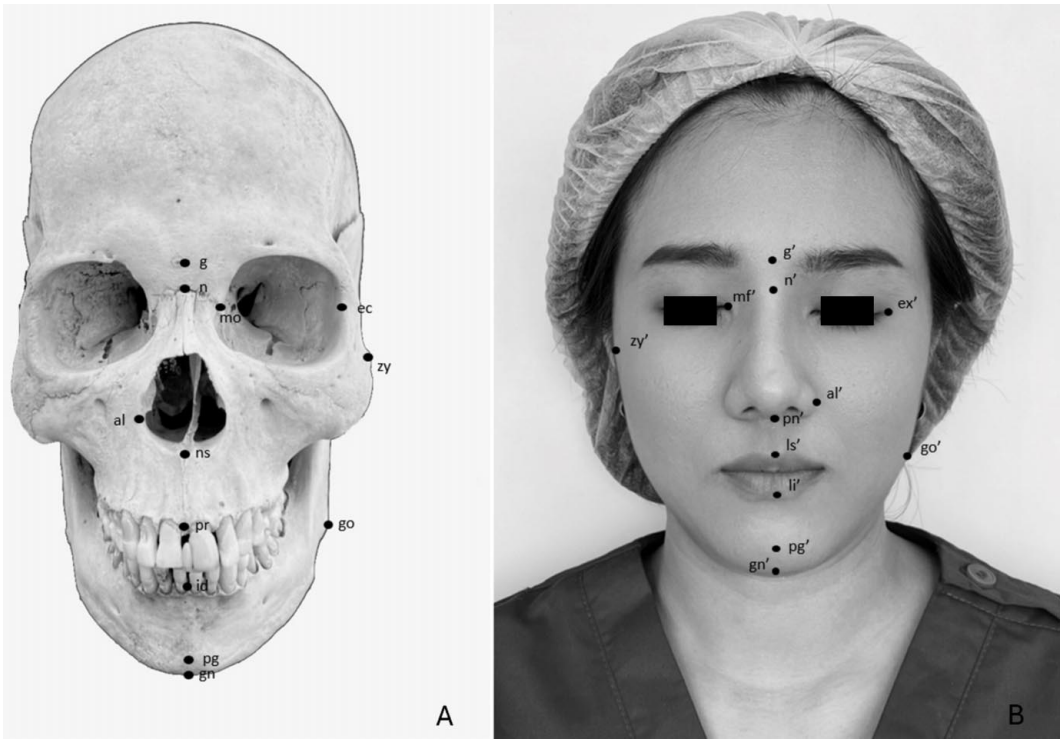

Fig. 1. (A) Craniometric landmarks for this research, (B) Facial landmarks for this research.

Image Transformation and Superimposition

In this study, image transformation for 2D–2D craniofacial superimposition involved scaling, rotation, and translation of the skull image relative to the facial image in the *x*–*y* plane. The transformation was expressed as a 3×3 matrix:

$$\begin{bmatrix} S_x cos\theta & 0(-sin\theta) & 0 \\ 0(cos\theta) & S_y sin\theta & 0 \\ T_x & T_y & 1 \end{bmatrix}$$

Where θ is the rotation angle, *Sx* and *Sy* are scaling factors, and *Tx* and *Ty* are translation. Following Ballerini *et al*. (2007), the transformed landmark coordinates (F') were calculated as:

$$F' = (S \cdot T \cdot P) \cdot C$$

with C representing the original skull landmarks.

A real-coded genetic algorithm (RCGA) was used to estimate transformation parameters. The algorithm was controlled by genetic processes such as selection, crossover, and mutation to minimize discrepancies between facial and cranial landmarks. This semi-automatic approach integrates expert-defined landmarks with computational optimization. The RCGA optimized five transformation variables: scaling along the *x* axis and *y* axis, rotation angle, and translation along the *x* axis and *y* axis.

The fitness function was designed to minimize anatomical landmark discrepancies by combining Euclidean distance and Curve registration. The mean square error (MSE) was first computed between facial landmarks and transformed skull landmarks:

$$MSE = \frac{\Sigma_{i=1}^{N}\sqrt{(x_{F\prime_i} - x_{F_i})^2 + (y_{F\prime_i} - y_{F_i})^2}}{N}$$

Where *N* is the number of landmarks. Additionally, curve registration (Sevaux & Mineur, 2005) was applied to align mandibular curvature between the gonial and pogonion points:

$$fitness = \sum_{i=0}^{N} (P_i - C(u_i))^2$$

Where: P_i is the curve point of the facial image.
$C(u_i)$ is the curve point of the skull that is nearest to the curve point of the facial image.

The final fitness function combined both components to guide the RCGA in determining the optimal transformation matrix.

Experiment method

The program's superimposition output demonstrates craniofacial alignments for 30 male and 40 female skull–face pairs with associated biological attributes. For each case, a blind test was conducted by comparing the facial image of one donor against four craniofacial superimpositions: one generated from the corresponding skull of the same individual and three generated from skulls of unrelated individuals. Accuracy assessment was performed using a least mean square error (MSE)–based algorithm to evaluate the four superimpositions per case.

Comparative analyses were conducted on the areas derived from craniometric and facial landmarks at the following positions: Nasion–Nasion', Nasospinale–Pronasale, Medial Orbit (R)–Maxillofrontale (R), and Medial Orbit (L)–Maxillofrontale (L) (Fig. 2A,B). The overall distances used for comparison are presented in Table II. Performance was evaluated using two different landmark sets: nine anatomical landmarks and seventeen anatomical landmarks. To determine statistically significant differences among individuals, a multivariate analysis of variance (MANOVA) was applied to the anatomical landmark measurements and inter-landmark distances.

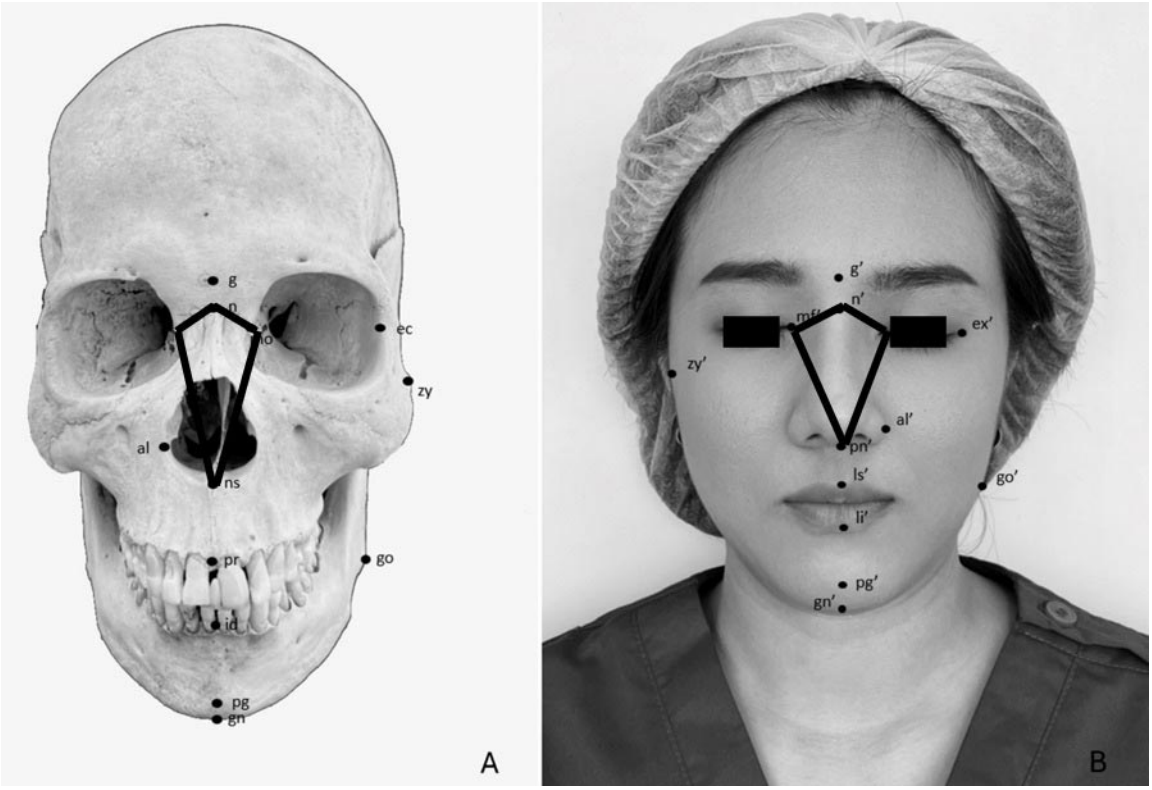

Fig. 2. (A) Craniometric landmarks used for area comparison, (B) Facial landmarks used for area comparison.

Table II. Distance of Anatomical Landmarks for comparison.

Craniometric landmarks	Facial landmarks
Glabella (g) - Nasion (n)	Glabella (g') - Nasion (n')
Nasion (n) - Nasospinale (ns)	Nasion (n') - Pronasale (pn')
Nasospinale (ns) - Prosthion (pr)	Pronasale (pn') - Labiale superius (ls')
Prosthion (pr) - Infradentale (id)	Labiale superius (ls') - Labiale inferius (li')
Infradentale (id) - Pogonion (pg)	Labiale inferius (li') - Pogonion (pg')
Pogonion (pg) - Gnathioin (gn)	Pogonion (pg') - Gnathion (gn')
Right Ectoconchion (ec R) – Right Medial Orbit (mo R)	Right Exocanthion (ex' R) – Right Maxillo frontale (mf' R)
Right Medial Orbit (mo R) – Left Medial Orbit (mo L)	Right Maxillo frontale (mf' R) - Left Maxillo frontale (mf' L)
Left Medial Orbit (mo L) - Left Ectoconchion (ec L)	Left Maxillo frontale (mf' L) - Left Exocanthion (ex' L)
Right Zygion (zy R) – Left Zygion (zy L)	Right Zygion (zy' R) – Left Zygion (zy' L)
Right Alare (al R) – Left Alare (al L)	Right Alare (al' R) – Left Alare (al' L)
Right Gonion (go R) – Left Gonion (go L)	Right Gonion (go' R) – Left Gonion (go' L)

RESULTS

From Table III, the accuracy of the data was evaluated using MSE, area comparison, and distance comparison for 9 and 17 anatomical landmark sets. Using 9 anatomical landmarks, males had mean accuracies of 43.33 % (MSE), 40 % (area), and 40 % (distance), with an overall average of 41.11 %. In females, they had corresponding values of 35 %, 45 %, and 35 % with an overall average of 38.33 %, respectively. Combined results yielded accuracy of 39.17 % (MSE), 42.5 % (area), and 37.5 % (distance). Males with 17 anatomical landmarks achieved consistent accuracies of 40 % for all three methods. Females achieved values of 30 % (MSE), 42.5 % (area) and 30 % (distance), and an overall average of 34.16 %. The combined male and female accuracy rates were 35 % (MSE), 41.25 % (area), and 35 % (distance). Therefore, the accuracy of using 9 anatomical landmarks was better than using 17 anatomical landmarks.

The results from analyzing differences in anatomical landmarks for superimposition using MANOVA indicate that *Hotelling's Trace Test* showed significant differences in males for both the use of 9 anatomical landmark ($p = 0.044$) and 17 anatomical landmark ($p = 0.047$) sets, while no significant differences were found in females ($p = 0.210$ and $p = 0.334$, respectively). Further analysis of individual landmarks revealed significant differences in males at the infradentale–labiale inferius, right zygion, and left zygion for the use of 9 anatomical landmarks sets, and at the infradentale–labiale inferius, pogonion, gnathion, and left zygion for the use of 17 anatomical landmarks sets. In females, no specific landmarks showed significant differences across either landmark set. Analysis was conducted with the p-value set at less than the significance level of 0.05 (Table IV).

The results from analyzing differences in anatomical landmarks for superimposition using MANOVA indicate that Hotelling's Trace Test showed no significant differences in both males and females for the 9 anatomical landmark sets ($p = 0.323$ and $p = 0.210$, respectively) and the 17 anatomical landmark sets ($p = 0.342$ and $p = 0.731$, respectively). Further analysis of individual landmarks revealed significant differences in males at the nasospinale–prosthion for both the use of 9 anatomical landmark sets and 17 anatomical landmark sets ($p < 0.001$). In females, no specific landmarks showed significant differences across either landmark set. The analysis was conducted with the p-value set at less than the significance level of 0.05 (Table V).

Table III. Summary of accuracy testing by Mean Square Error (MSE), Area comparison and Distance Comparison.

	Accuracy testing by the Mean Square Error (MSE), Area comparison and Distance Comparison							
	9 Anatomical Landmarks				17 Anatomical Landmarks			
	Mean Square Error (MSE)	Area comparison	Distance comparison	Summary of 3 testing	Mean Square Error (MSE)	Area comparison	Distance comparison	Summary of 3 testing
Male (30)	43.33 %	40 %	40 %	41.11 %	40 %	40 %	40 %	40 %
Female (40)	35 %	45 %	35 %	38.33 %	30 %	42.50 %	30 %	34.16 %
Summary of Male and Female	39.165 %	42.5 %	37.5 %		35 %	41.25 %	35 %	

Table IV. Multivariate test of MSE in each landmark ($p < 0.05$).

	9 Anatomical Landmarks		17 Anatomical	
	Male p-value	Female p-value	Male p-value	Female p-value
Multivariate Test				
Hotelling's Trace	**0.044**	0.210	**0.047**	0.334
Anatomical Landmarks				
Glabella - Glabella'	0.108	0.416	0.133	0.407
Nasion - Nasion'	0.796	0.600	0.858	0.665
Nasospinale - Pronasale	0.557	0.436	0.053	0.323
Prosthion - Labiale superius	0.219	0.357	0.844	0.092
Infradentale - Labiale inferius	**0.001**	0.979	**0.012**	0.827
Zygion(R) - Zygion'(R)	**0.021**	0.204	0.329	0.144
Zygion(L) - Zygion'(L)	**0.002**	0.614	0.141	0.079
Alare(R) - Alare'(R)	0.952	0.568	0.243	0.498
Alare(L) - Alare'(L)	0.284	0.496	0.684	0.890
Pogonion - Pogonion'	-	-	**0.001**	0.988
Gnathion - Gnathion'	-	-	**0.002**	0.944
Ectoconchion(R) - Exocanthion(R)	-	-	0.314	0.085
Medial Orbit (R) - Maxillo frontale (R)	-	-	0.643	0.415
Ectoconchion(L) - Exocanthion(L)	-	-	0.199	0.443
Medial Orbit (L) - Maxillo frontale (L)	-	-	0.501	0.165
Gonion(R) - Gonion'(R)	-	-	0.322	0.718
Gonion(L) - Gonion'(L)	-	-	0.751	0.149

Table V. Multivariate test of distance comparison in each landmark ($p < 0.05$).

		9 Anatomical Landmarks		17 Anatomical Landmarks	
		Male p-value	Female p-value	Male p-value	Female p-value
Multivariate Test					
Hotelling's Trace		0.323	0.210	0.342	0.731
Craniometric distance	**Facial distance**				
Glabella(g) - Nasion(n)	Glabella(g') - Nasion(n')	0.382	0.949	0.390	0.921
Nasion(n) - Nasospinale(ns)	Nasion(n') - Pronasale(pn')	0.776	0.149	0.761	0.121
Nasospinale(ns) - Prosthion(pr)	Pronasale(pn') - Labiale superius(ls')	**0.000**	0.531	**0.000**	0.415
Prosthion(pr) - Infradentale(id)	Labiale superius(ls') - Labiale inferius(li')	0.214	0.913	0.287	0.916
Infradentale(id) - Pogonion(pg)	Labiale inferius(li') - Pogonion(pg')	0.969	0.785	0.946	0.790
Pogonion(pg) - Gnathioin(gn)	Pogonion(pg') - Gnathion(gn')	0.712	0.983	0.758	0.982
Right Ectoconchion(ecR) - Right Medial Orbit(moR)	Right Exocanthion(ex'R) - Right Maxillo frontale(mf'R)	0.969	0.772	0.970	0.776
Right Medial Orbit(moR) - Left Medial Orbit(moL)	Right Maxillo frontale (mf'R) - Left Maxillo frontale (mf'L)	0.809	0.203	0.841	0.201
Left Medial Orbit(moL) - Left Ectoconchion(ecL)	Left Maxillo frontale(mf'L) - Left Exocanthion(ex'L)	0.770	0.146	0.820	0.152
Right Zygion(zyR) - Left Zygion(zyL)	Right Zygion(zy'R) - Left Zygion(zy'L)	0.588	0.232	0.598	0.241
Right Alare(alR) - Left Alare(alL)	Right Alare(al'R) - Left Alare(al'L)	0.960	0.649	0.961	0.648
Right Gonion(goR) - Left Gonion(goL)	Right Gonion(go'R) - Left Gonion(go'L)	0.839	0.731	0.824	0.763

DISCUSSION

This research evaluated the application of a semi-automatic craniofacial superimposition procedure with two groups of anatomical landmarks. In general, the 9 anatomical landmark sets performed slightly better than the 17 anatomical landmark sets, producing higher and more consistent accuracy, especially in males. Using fewer but more dependable points seems to decrease the variability of unstable landmarks and to simplify the computation for the method. Similar results have been confirmed in previous studies that stressed the value of reproducible landmarks rather than simply increasing their number (Nickerson *et al*., 1991; Ballerini *et al*., 2007; Caple & Stephan, 2016). Results in this research also support the value of applying optimization techniques such as genetic algorithms to reduce operator bias and improve objectivity.

Regarding the types of evaluation, area-based analysis yielded the greatest accuracy, which was especially relevant for females, where the accuracy of area comparison clearly outperformed both MSE and distance-based approaches. This observation indicates that area measurements may react more strongly to subtle craniofacial congruence when skeletal features are less prominent. In males, the outcomes from all three methods were similar, suggesting that pronounced skeletal structures facilitate a stabilization of performance across measures. Distance measures were useful but consistently less accurate than area analysis, indicating their lack of capacity to account for the full spatial relationships.

These MANOVA results showed distinct sex-specific differences. In males, considerable differences were noted among both landmark sets, notably at the infradentale–labiale inferius, zygion, pogonion, and gnathion. In contrast, there were no significant differences in magnitude at the overall or landmark level for females. The results agree with sexual dimorphism pattern data: male skulls have generally greater mandibular and zygomatic morphology, which seems to be more sensitive to misalignment during craniofacial superimposition. It is further supported by differences at the gonion and zygion, whereby the angularity and curvature of the male mandible along with the robustness of the zygomatic arches, may improve skeletal definition yet predispose it to positional mismatch when compared to facial images. This is perhaps a result of the smoother contours that are characteristic of female cranial morphology, perhaps a contributing factor to the lack of substantial differences between cohorts of men and women. Distance-based analysis also revealed the midface to be a significant region with significant differences at the nasospinale–prosthion in males ($p < 0.001$).

Another factor contributing to these changes is age-associated change. Photographs in this study tended to show people in early adulthood, with skulls showing advanced age too. Mendelson & Wong (2020) pointed out that age is associated with specific skeletal changes: resorption of the maxilla, piriform aperture, and orbital rims, along with changes to the mandible. These, along with soft tissue atrophy, skin laxity, and dental loss, can cause enormous discrepancy between the youthful photographs and those of older skeletal bodies. Such differences may contribute to some of the variability reported in this analysis and highlight the need to incorporate age-adjusted morphology or computational modeling of facial aging techniques.

This study is relatively limited in its use of 2D images. 2D images only provide a 2D view and cannot depict the 3D depth and curvature of the craniofacial structure; thereby, introducing landmarks in highly complicated locations such as orbital rims, zygion, and gonion. The risk increases with photographic characteristics including angle, lighting, and image quality. Some photographs applied in this study were archival without metadata, as focal length, lens distortion, or photographic setting details were not included. The absence of this information makes standardizing scale and orientation challenging, which could cause additional mistakes. 2D methods also exhibit volumetric inaccuracy and miss contextual information present in the image relative to more recent 3D superimposition techniques that might compromise applicability to forensic tasks.

2D images also have many practical advantages. Contrary to CT-derived 3D approaches based on more sophisticated tools that are not available in most locations, 2D approaches are also suitable for a large number of conventional photographs. 2D superimposition is especially attractive in low-resource forensic contexts where CT scanners and advanced imaging materials are scarce. There is also great encouragement that readily available images can be employed, as the techniques are easily used for other forensic purposes and extend beyond the confines of dedicated labs. The results are all important for the field of craniofacial superimposition because they indicate the need for targeted landmark selection, the relative importance of various accuracy measures, the effects of sex and age, and the technical limitations of 2D images. They also support the use of computational optimization to improve objectivity. Thus, such findings would assist in identification when forensic practitioners lack essential identifiers, such as DNA, fingerprints, or dental records.

CONCLUSION

This study reports a semi-automatic operation of craniofacial superimposition using genetic algorithms and an anatomical landmark-based optimization approach. They find that fewer well-selected anatomical landmarks are typically selected more reliable and consistent than larger ones. Thus, the study provides a rationale for the selection of anatomical landmarks. This insight not only leads to enhanced computational efficiency but is also reproducible, which serves as a key requirement for forensic applications.

Among the evaluation methods, area-based analysis emerged as the most significant, which indicated an accurate measure of the effectiveness of craniofacial congruence. The implementation of computational optimization facilitated the reduction of operator bias and the implementation of an increasingly standardized and objective system. Taken together, these elements contribute to a methodological approach that can support and improve the validity of craniofacial superimposition as a forensic identification technique.

While there are limitations of a 2D image, it provides a tremendous advantage to the accessibility of the method. Unlike 3D methodologies that need costly and technical applications, the generalizability of standard photographic material to various forensic settings, especially those where resources are scarce, supports broader use. This availability is important to assert that craniofacial superimposition continues to be an effective and legitimate solution when primary markers such as DNA, fingerprints, or dental findings are not available.

This research enriches the implementation of craniofacial superimposition through demonstration of the optimal use of landmark selection, optimization of computation, and choice of sensitive evaluation quantification procedures with high accuracy and objectivity. Such efforts reinforce craniofacial superimposition as an available, dependable, and scientifically substantiated method within the field of forensic identification.

ACKNOWLEDGEMENTS.

We would like to thank the Excellence Center in Osteology Research and Training Center, Faculty of Medicine, Chiang Mai University, Chiang Mai, Thailand for their support.

SRISINGHASONGKRAM, J.; PALEE, P.; MONUM, T.; PRASITWATTANASEREE, S.; IAMAROON, A. I. & MAHAKKANUKRAUH, P. Eficacia de los puntos de referencia craneométricos y faciales para la superposición craneofacial mediante algoritmos genéticos en una población tailandesa. *Int. J. Morphol., 44(1)*:121-129, 2026.

RESUMEN: La superposición craneofacial ha sido una herramienta forense eficaz para la identificación humana cuando no se dispone de identificadores primarios como el ADN, las huellas dactilares o los registros dentales. En este estudio, se utiliza un método semiautomatizado que combina un algoritmo genético con codificación real y una optimización basada en puntos de referencia aplicada a 30 pares cráneo-cara masculinos y 40 femeninos. Para la precisión, se evaluaron el error cuadrático medio (ECM), el área y la distancia en dos conjuntos de puntos de referencia (nueve y diecisiete puntos). El conjunto de nueve puntos de referencia obtuvo resultados mejores y más consistentes (41,11 % en hombres; 38,33 % en mujeres) que el conjunto de diecisiete puntos de referencia (40 % y 34,16 %, respectivamente). La evaluación basada en áreas mostró la menor diferencia y la mayor precisión, específicamente en mujeres, y MANOVA demostró diferencias significativas solo en hombres en los puntos de referencia mandibulares y cigomáticos. Con base en estos resultados, un conjunto más pequeño de puntos de referencia, pero más apropiado, aumenta tanto la precisión como la eficiencia computacional, mientras que las métricas basadas en áreas son las más significativas. Sin embargo, considerando las limitaciones de los datos bidimensionales, la técnica sigue siendo viable en entornos con recursos limitados, lo que respalda la superposición craneofacial como una forma confiable de identificación forense.

PALABRAS CLAVE: Superposición craneofacial; Cráneo; Antropología forense; Algoritmo genético.

REFERENCES

Ballerini, L.; Cordón, Ó.; Damas, S.; Santamaria, J.; Aleman, I. & Botella, M. *Craniofacial Superimposition in Forensic Identification using Genetic Algorithms.* In: Proc. 3rd Int. Symp. Inf. Assur. Secur. (IAS 2007). IEEE; 2009. pp.429-34.

Barut, C. & Ertilav, H. Guidelines for standard photography in gross and clinical anatomy. *Anat. Sci. Educ., 4(6)*:348-56, 2011.

Buikstra, J. E. & Ubelaker, D. H. *Measurement in Adult Remains*. In: Buikstra, J. E. & Ubelaker, D. H. (Eds.). Standards for Data Collection from Human Skeletal Remains. Fayetteville, Arkansas Archeological Survey, 1994.

Caple, J. & Stephan, C. N. A standardized nomenclature for craniofacial and facial anthropometry. *Int. J. Legal Med., 130(3)*:863-79, 2016.

Damas, S.; Cordón, O. & Ibáñez, O. *MEPROCS Craniofacial Superimposition Framework*. In: Damas, S.; Cordón, O. & Ibáñez, O. (Eds.). Handbook on Craniofacial Superimposition. The MEPROCS Project. Cham, Springer, 2020. pp.139-52.

Mendelson, B. & Wong, C. H. Changes in the facial skeleton with aging: implications and clinical applications in facial rejuvenation. *Aesthet. Plast. Surg., 44(4)*:1159-61, 2020.

Nickerson, B.; Fitzhorn, P.; Koch, S. & Charney, M. A methodology for near-optimal computational superimposition of two-dimensional digital facial photographs and three-dimensional cranial surface meshes. *J. Forensic Sci., 36(2)*:480-500, 1991.

Okeson, J. P. *Functional anatomy and biomechanics of the masticatory system*. In: Management of Temporomandibular Disorders and Occlusion. Kentucky, Elsevier, 2020.

Ricci, A.; Marella, G. L. & Apostol, M. A. A new experimental approach to computer-aided face/skull identification in forensic anthropology. *Am. J. Forensic Med. Pathol., 27(1)*:46-9, 2006.

Sevaux, M. & Mineur, Y. A curve-fitting genetic algorithm for a styling application. *Eur. J. Oper. Res., 179(3)*:895-905, 2007.

Srisinghasongkram, J.; Mahacharoen, T.; Singsuwan, P. & Mahakkanukrauh, P. Preliminary study of craniofacial superimposition by mathematics programming in a Thai population. *Med. Health, 14(2)*:235-41, 2019.

Tan, J. S.; Liao, I. Y.; Venkat, I.; Belaton, B. & Jayaprakash, P. T. Computer-aided superimposition via reconstructing and matching 3D faces to 3D skulls for forensic craniofacial identifications. *Vis. Comput., 36*:1739-53, 2020.

Taylor, J. A. & Brown, K. A. *Superimposition Techniques: Introduction*. In: Clement, J. G. & Ranson, D. L. (Eds.). Craniofacial Identification In Forensic Medicine. New York, Oxford University Press, 1998.

Ubelaker, D. H. & Scammell, H. *Bones, A Forensic Detective's Casebook.* New York, Harper Collins, 1992.

Yuvaraj, N.; Kousik, N.; Arshath Raja, R. & Saravanan, M. Automatic skull-face overlay and mandible articulation in data science by AIRS-genetic algorithm. *Int. J. Intell. Netw., 1*:9-16, 2020.

Corresponding author:
Prof. Pasuk Mahakkanukrauh, MD
Research Cluster in Osteology Research and Training Center (ORTC)
Chiang Mai University
Chiang Mai 50200
THAILAND

E-mail: pasuk034@gmail.com